Korean J. of Chem. Eng., **13**(6), 620-626 (1996)

KINETICS OF FORMATION OF CARBON DIOXIDE CLATHRATE HYDRATES

Moon-Kyoon Chun and Huen Lee†

Dept. of Chemical Engineering, Korea Advanced Institute of Science and Technology,
373-1 Kusong-dong, Yusong-gu, Taejon 305-701, Korea
(Received 25 June 1996 • accepted 29 August 1996)

Abstract – The new experimental apparatus capable of observing the clathrate hydrate formation kinetics was developed in this study. Experimental data on the kinetics of carbon dioxide hydrate formation were carefully measured. The experiments were carried out in a semi-batch stirred tank reactor with stirring rate of 500 rpm at three different temperatures between 275.2 and 279.2 K and at pressures ranging from 2.0 to 3.5 MPa. The kinetic model was adopted to predict the growth of hydrates with only one adjustable parameter which represented the rate constant for the hydrate particle growth. The model was based on the crystallization theory coupled with the two-film theory for gas absorption into the liquid phase. The model predictions matched the experimental data very well with the largest deviation of 7.18%, which is within experimental error range. This study is the first for the kinetic data of carbon dioxide hydrate formation and important in developing carbon dioxide fixation process using clathrate hydrate phenomenon.

Key words : Kinetics, Carbon Dioxide, Hydrate, Clathrate, Crystallization

INTRODUCTION

Clathrate hydrates are crystalline compounds formed from guest molecules and host water molecules under suitable conditions of temperature and pressure. The water molecules are linked together with hydrogen bonds and form a three-dimensional structure containing cavities capable of entrapping guest molecules. The hydrate structure is stabilized only through the physical interaction between the encaged gas molecules and the water lattice. It has been recognized that the plugging problem of gas pipelines in natural gas transportation was primarily due to the gas hydrate formation between water and natural gases composed of methane, ethane, propane, and other light hydrocarbon. The phase behavior of the gas hydrate formation has been of considerable significance to the natural gas industry. On the other hand the gas hydrate formation has offered the possibility for the development of a seawater desalination process and gas storage and separation processes. Detailed information on the structural and physical properties of gas hydrates can be found in the literature [Sloan, 1990; Berecz and Balla-Achs, 1983].

Although the thermodynamics of gas hydrates have been studied extensively for more than three decades, the kinetics of formation and decomposition have only recently been investigated. Vysniauskas and Bishnoi [1983, 1985] reported data on the kinetics of methane and ethane hydrates formation and proposed a semi-empirical model in order to correlate the data. Their studies were the first attempt to describe quantitatively and model the formation kinetics of gas hydrates which were taken by contacting gas with water at temperatures above the freezing point of water. The kinetics of gas hydrate decomposition have also been studied recently by Kim et al. [1987]. Englezos et al. [1987a] studied the kinetics of methane and ethane hydrate formation and proposed a mechanistic model for the formation kinetics, with only one adjustable parameter representing the rate constant for the hydrate particle growth. Their kinetic model was based on the crystallization theory, while the two-film theory model was adopted for the interfacial mass transfer. They also extended the model to the formation of hydrates from mixtures of methane and ethane [Englezos et al., 1987b]. Jamaluddin et al. [1989] developed a mathematical model to predict the rate of decomposition of a synthetic gas hydrate block by coupling intrinsic kinetics with the heat transfer rates. Dholabhai et al. [1993] reported data on the kinetics of methane hydrate formation in aqueous electrolyte solutions and adapted the kinetic model developed by Englezos et al. [1987a] to predict the growth of hydrates.

Global warming induced by carbon dioxide and other greenhouse gases is a serious problem for mankind. Carbon dioxide is the most important greenhouse gas from human activities. Increase in carbon dioxide concentrations in the atmosphere contribute over half of the enhanced greenhouse effect, the rest being mainly due to increases in halocarbons and methane. The disposal and sequestration of CO_2 in the deep ocean has been considered as a potential strategy for reducing atmospheric concentrations of this greenhouse gas species as a means to mitigate global warming. Modeling this process has been complicated by insufficient understanding of the complex transport and chemical kinetics of the system. There were a few studies on modeling of kinetics of carbon dioxide hydrate formation. Saji et al. [1992] studied the disposal of carbon dioxide into the deep sea by the formation of clathrate hydrate. They reported experiments of equilibrium and kinetics of carbon dioxide hydrate formation. Shindo et al. [1993a, b] developed a one-

†To whom all correspondences should be addressed.

dimensional kinetic model for hydrate formation at the interface between adjacent semi-infinite reservoirs of liquid CO_2 and water. They concluded that hydrate would form very rapidly and that the hydrate layer would be very thin. Lund et al. [1994] developed a dynamic model for formation and stability of CO_2-hydrate on the interface of liquid CO_2 and ocean water at large depths. Teng et al. [1995] studied a kinetic model of hydrate formation on the surface of a CO_2 droplet in high-pressure, low-temperature water. Their model predicted that the hydrate layer formed was very thin and that the formation time was less than two seconds.

In the present study, experimental data on the kinetics of carbon dioxide hydrate formation in water solution were obtained. The equipment and the experimental procedure used were newly developed in this study. In order to guarantee the validity of the experimental apparatus, a preliminary test was performed for the methane hydrate system. The experiments were carried out under isothermal and isobaric conditions to measure the consumption rate of carbon dioxide after nucleation had commenced. The nucleation was initially identified by the visual observation of turbidity in the aqueous solution. The kinetic model developed by Englezos et al. [1987a], which is based on the theory of crystallization, is adopted to predict the experimental data of kinetics of carbon dioxide hydrate formation.

KINETIC MODEL

The model developed by Englezos et al. [1987a] for hydrate growth in pure water was adopted to this study. The formation of gas hydrates was viewed as a crystallization process by Englezos et al. and it was first attempt to model it according to the kinetics of crystallization. According to them, hydrate formation is a phase transformation which requires a supersaturated environment in order to occur. Gas molecules dissolved in liquid water build the supersaturated environment, throughout the liquid phase or locally near the interface. At some point during the dissolution (turbidity point), the precursors to the hydrate phase (nuclei) appear. The nuclei subsequently grow if sufficient gas is present in the structured water environment. The particulate nature of the process implies that two distinct kinetic processes (nucleation and growth) are involved and they have to be coupled with the transport processes to describe the overall phenomenon. Nucleation and growth occur predominantly on the gas-water contact interface, where the supersaturation is higher than anywhere else in the liquid water phase. The type of nucleation is primary or spontaneous homogeneous (absence of foreign particles) nucleation. For modeling the data, it is assumed that the nuclei are formed instantaneously and after the turbidity the primarily nucleation ceases because the energy barrier to form a new nucleus is greater than that of the enclathration of gas into existing nucleation centers. They proposed that the overall driving force for the crystallization process be given by the difference in the fugacity of the dissolved gas and the three-phase equilibrium fugacity at the experimental temperature:

$$\Delta f = f - f_{eq}. \tag{1}$$

The model considers the growth of hydrate particles as two consecutive step processes (diffusion and reaction) and uses the two-film theory to describe the absorption of the gas at the gas-liquid interface. As shown in Fig. 1, each particle, which is assumed to be spherical, is surrounded by an adsorption reaction layer followed by a stagnant diffusion layer. Particles could be located either in the liquid film at the gas-liquid interface or in the bulk of the solution. The dissolved gas diffuses from the solution surrounding the stagnant layer to the hydrate particle-water interface and, then, by an adsorption process, the gas molecules are incorporated into the structured water framework. The driving forces for the diffusion around the particles is $(f - f_s)$ whereas it is $(f_s - f_{eq})$ for the reaction step. At steady state, the rates of the two steps are equal and, therefore, f_s can be eliminated from the individual rate expressions to yield the rate of growth per particle:

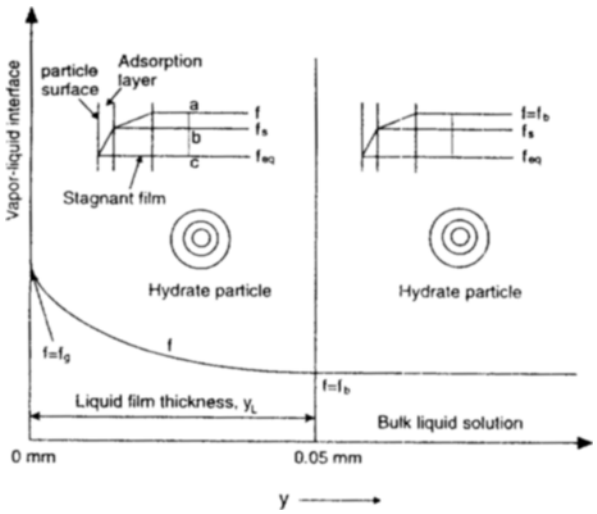

Fig. 1. Schematic representation of the fugacity of CO_2 in the liquid and around a particle. ab and bc are the driving forces for diffusion and reaction, respectively.

$$\left(\frac{dn}{dt}\right)_p = K^* A_p \left(f - f_{eq}\right) \tag{2}$$

The quantity, $(f - f_{eq})$, which is the difference in the fugacity of the dissolved gas and its fugacity at the three phase equilibrium, defines the overall driving force. K^* is the combined rate constant for the diffusion and adsorption processes and A_p is the surface area of each particle. A global reaction rate for all the particles is given by

$$R_v(t) = \int_0^\infty \left(\frac{dn}{dt}\right)_p \phi(r, t)dt = \int_0^\infty K^* A_p (f - f_{eq})\phi(r, t)dr$$
$$= 4\pi K^* \mu_2 (f - f_{eq}) \tag{3}$$

where $\phi(r, t)$ is the particle size distribution and μ_2 is the second moment of the particle size distribution

$$\mu_2 = \int_0^\infty r^2 \phi(r, t)dr. \tag{4}$$

Therefore, the global reaction rate can be written in the form

$$R_v(t) = K(f - f_{eq}). \tag{5}$$

The rate of the crystallization process taking place in the liquid phase is thus described by the overall rate given by Eq. (5), i.e., a pseudo-first-order irreversible homogeneous reaction.

Following the development of Englezos et al. [1987a], the five differential equations, Eq. (6) to (10), with their initial conditions constitute the governing equations which describe the dynamic behavior of the physical system.

$$\frac{dn}{dt}=\left(\frac{D^*\gamma A_{(g-l)}}{yL}\right)\frac{[(f_g-f_{eq})\cosh\gamma-(f_b-f_{eq})]}{\sinh\gamma},\quad n(0)=n_{tb} \tag{6}$$

$$\frac{df_b}{dt}=\frac{HD^*\gamma a}{c_{w0}y_L\sinh\gamma}\left\{(f_g-f_{eq})-(f-f_{eq})\cosh\gamma\right\}-\frac{4\pi K^*\mu_2 H(f_b-f_{eq})}{c_{w0}},\quad f_b(0)=f_{eq} \tag{7}$$

$$\frac{d\mu_0}{dt}=\alpha_2\mu_2,\qquad \mu_0(0)=\mu_0^0 \tag{8}$$

$$\frac{d\mu_1}{dt}=G\mu_0,\qquad \mu_1(0)=\mu_1^0 \tag{9}$$

$$\frac{d\mu_2}{dt}=2G\mu_1,\qquad \mu_2(0)=\mu_2^0 \tag{10}$$

In the derivation of the above equations it is assumed that the liquid phase volume and the number of moles of water remain practically constant and that the moles of the gas dissolved are negligible compared to the water moles. α_2 is the secondary nucleation constant and γ is the Hatta number:

$$\gamma=y_L(4\pi K^*\mu_2/D^*)^{1/2} \tag{11}$$

D^* is given by

$$D^*=\frac{Dc_{w0}}{H} \tag{12}$$

An average growth rate required for the computation of the first and second moments can be defined as follows:

$$G_{avg}=\left(\frac{1}{L}\right)\left[\int_0^{y_L}\left(\frac{dr}{dt}\right)dy+\left(\frac{dr}{dt}\right)_b(L-y_L)\right] \tag{13}$$

where the linear growth rate is given by

$$\frac{dr}{dt}=\frac{K^*M(f-f_{eq})}{\rho}. \tag{14}$$

Upon substitution into Eq. (13),

$$G_{avg}=\left(\frac{K^*M}{\rho_l}\right)\times\left(y_L\frac{(f_g+f_b-2f_{eq})(\cosh\gamma-1)}{\gamma\sinh\gamma}+(L-y_L)(f_b-f_{eq})\right). \tag{15}$$

The initial condition for Eq. (6) is the number of moles of the gas transported into the aqueous phase up to the "turbidity point". This is available from the experimental data. It is assumed in the model that at the turbidity point the fugacity of the gas in the bulk aqueous phase instantaneously drops to the three-phase equilibrium value. This defines the initial condition for Eq. (7). The number of particles per unit volume of the aqueous phase at turbidity, μ_0^0, is computed from the moles of the gas dissolved just prior to the appearance of the hydrates and the critical radius of the nucleus. If n_{tb} is the amount of gas consumed that has been dissolved up to the turbidity point, then the gas consumed for hydrate formation is $n_{tb}-n_{eq}$, where n_{eq} is the amount of gas that would have been dissolved at the three-phase equilibrium pressure and experimental temperature. The critical radius of the nucleus is given by

$$r_{cr}=-\frac{2\sigma}{\Delta g}. \tag{16}$$

The free energy per unit volume of the product formed, Δg, and the number of particles per unit volume are given by

$$-\Delta g=\left(\frac{RT_{exp}}{v_m}\right)\left(\ln\frac{f_b}{f_{eq}}+\frac{n_w v_w(P_{exp}-P_{eq})}{RT_{exp}}\right) \tag{17}$$

and

$$\mu_0^0=\frac{3M(n_{tb}-n_{eq})}{4\pi V_L\rho r_{cr}^3} \tag{18}$$

The initial conditions for the other two moments of the particle size distribution are

$$\mu_1^0=2r_{cr}\mu_0^0 \tag{19}$$

$$\mu_2^0=4r_{cr}^2\mu_0^0 \tag{20}$$

Diffusivities for methane and carbon dioxide are calculated based on the Wilke and Chang correlation with improved parameters, given by Hayduk and Laudie [1974]. Gas-phase fugacities are calculated using the Peng-Robinson equation of state [Peng and Robinson, 1976]. The film thickness, y_L, is obtained from

$$y_L=\frac{D}{k_l}=\frac{Da}{(k_L a)} \tag{21}$$

The values of $k_L a$ and Henry's constant are determined from the solubility experiments.

The experimental data were used to determine the only unknown parameter, the combined rate constant, K^*, in the model by minimizing the difference between the model predictions and the measurements of the moles of gas consumed during hydrate formation. Differential equations, Eq. (6) to (10), along with their initial conditions were solved simultaneously using IMSL's IVPAG differential equation solver. All the model parameters are determined *a priori*.

EXPERIMENTAL

1. Apparatus and Materials

The experimental apparatus was designed to measure the volumetric consumption rate of a hydrate-forming gas during hydrate formation which is the most important variable in the kinetic study. A schematic diagram of the experimental apparatus is shown in Fig. 2. It consists of a semi-batch stirred tank

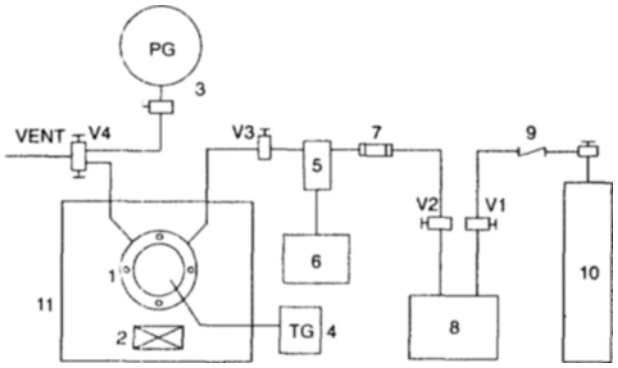

Fig. 2. Experimental apparatus for clathrate hydrate kinetics.

1. Reactor
2. Magnetic stirrer
3. Pressure gauge
4. Thermometer
5. Flowmeter
6. Data acquisition system
7. Check valve
8. Micro flow syringe pump
9. Line filter
10. Gas cylinder
11. Constant temperature water bath

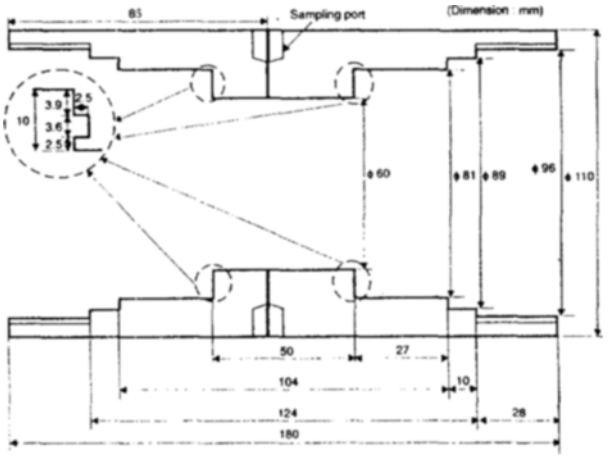

Fig. 3. Schematic diagram of reactor for clathrate hydrate kinetics.

reactor with a temperature control system, a micro flow syringe pump to supply hydrate-forming gas to the reactor and to control the reactor pressure, a mass flowmeter to measure the flowrate of gas, and the accompanying data acquisition system. The cylindrical type reactor shown in Fig. 3 was made of 316 stainless steel with two sight glasses equipped at the front and back of the reactor. These sight glasses provided visual observation of hydrate formation inside the reactor during nucleation and were perfectly sealed by rubber *o*-rings. The cylindrical cavity of reactor had an internal volume of about 140 cm^3. Water charged in the reactor was vigorously agitated by a magnetic spin bar with an external magnet immersed in a water bath. The magnetic stirrer (Cole-Parmer, H-04650-62) had a built-in frequency generator which provides a stable speed control for the range of 200 to 1400 rpm. The temperature of the reactor was controlled by an externally circulating refrigerator/heater. The actual temperature in the reactor could be measured by the K-type thermocouple with a digital thermometer (Cole-Parmer, 8535-26) of which the resolution was ± 0.1 K. This thermometer was calibrated with the ASTM D900 mercury thermometer. The pressure of the system was initially supplied from a gas cylinder (1), after which the pressure was controlled by a micro flow syringe pump (ISCO, μLC-500, 1240-018) operated at constant pressure mode. The pressure range of a micro flow syringe pump was 0.10 to 70.00 MPa of which the resolution was $\pm 2\%$ of full-scale. The pressure in the reactor was kept constant by using constant pressure mode of the micro flow syringe pump, while the hydrate-forming gas flow rate varied during the hydrate-formation reaction. A Heise gauge (CMM 44307, 0 to 20.0 MPa range) having the maximum error of $\pm$ 0.01 MPa was used to measure the reactor pressure. The mass flowmeter (OMEGA, FMA-8500) was used to obtain the amount of gas consumed during the hydrate formation which allowed accurate measurement of the mass flow rate of hydrate-forming gas. The mass flowmeter produced a 0-5 Vdc output signal linear to the mass flow rate which is equivalent to the range from 0 to 10 ml/min with an accuracy of $\pm 1\%$ of full scale. The personal computer was used for direct data acquisition of the mass flowrate of the gas and to perform on-line calculations of the gas consumption throughout an experiment. The methane with a purity of 99.9 mol% and the carbon dioxide with a minimum purity of 99.99 mol%, supplied by World Gas Inc., were used. The double-distilled and deionized water was used.

2. Procedure

The hydrate formation kinetics were observed by contacting hydrate-forming gas with water in the semi-batch stirred tank reactor at constant temperature and pressure conditions. When the gas in the reactor was consumed in order to produce hydrate crystals, a micro flow syringe pump automatically provided additional gas for the reactor to maintain constant pressure conditions. The flow rate of the supplied gas to the reactor was directly measured by a mass flowmeter. The voltage signals generated by the mass flowmeter were transferred to a PC based data acquisition system and then converted to the volumetric consumption rate of the gas at standard conditions of 293.2 K and 1 atm.

The kinetic experiment on the hydrate formation was first prepared by charging the reactor with double-distilled and deionized water. The reactor was then pressurized to a pressure of about 0.05 MPa below the equilibrium pressure for the hydrate formation at the specified experimental temperature. Throughout stirring the water charged in the reactor vigorously for approximately 30 min, the water sample was then saturated with the hydrate-forming gas. No further pressure change indicated the saturation of the water sample. When the saturation of the water was attained the stirring of the water was stopped. After the valves V2 and V3 were opened, the reactor was pressurized to the experimental pressure and allowed to reach the constant experimental temperature. When thermal equilibrium was obtained in the system the stirring of the water sample was started again. The reactor was under automatic control and the data acquisition from the mass flowmeter was commenced. During the reaction the amount of the gas consumed for the formation of hydrate was automatically supplemented by the micro flow syringe pump. The flow rate of the supplied gas equivalent to the consumption rate of the gas in the reactor was directly measured by the mass flowmeter mounted between the reactor and the micro flow syringe pump. The vol-

tage signal generated by the mass flowmeter was linear to gas flow rate and converted to the volumetric flow rate of the gas at standard conditions of 293.2 K and 1 atm by the on-line data acquisition system. The kinetic experiments were performed until the magnetic spin bar was stopped. All the experiments were conducted at 500 rpm except for the kinetics of methane hydrate formation with the stirring rate of 400 rpm.

The calibration of the mass flowmeter at each pressure was performed by using the capillary flowmeter (HP, 9301-1199) at standard conditions. The capillary flowmeter digitally displayed the flow rate ranging from 0.1 to 50.0 ml/min with an accuracy of $\pm 3\%$ of reading.

RESULTS AND DISCUSSION

The new experimental apparatus capable of observing the formation kinetics of clathrate hydrate was developed in this study. Several preliminary tests were performed to check the validity of the experimental apparatus. The experimental kinetic data of carbon dioxide hydrate formation and the estimated consumption curves by the kinetic model developed by Englezos et al. were obtained.

In order to establish the validity of the experimental setup, the experimental data of methane hydrate kinetics after the turbidity point at 276 K and 4.86 MPa were compared with the data available in the literature [Englezos et al., 1987a]. The experimental data obtained in the present work together with the literature data were shown in Fig. 4. Both data almost coincide until the initial 10 minutes. Since there were few hydrate particles and the size of them was small during the initial period of hydrate formation, the consumption rate of the gas was shown to be dependent on the number and size of hydrate particles according to the similarity of both data. The difference between two data sets became larger as the hydrate formation continued. This may be caused by the difference of geometrical shape of the reactor employed, i.e., the difference of interfacial area per unit volume of the aqueous phase. The interfacial areas per unit volume obtained in this work and the previous work were 197.2 m^2/m^3 and 42.6 m^2/m^3, respectively. As the time elapsed, hydrate particles were growing larger and the number of particles continuously increased. The consumption rate of the hydrate-forming gas could be largely dependent on the interfacial area per unit volume of gas and liquid phases. The CH_4 consumption rate for the methane hydrate formation in the present reactor cell was shown to be higher than that in the previous work. This result indicates that the reactor shape of this study has a better condition for the methane hydrate crystal formation.

The reproducibility test of carbon dioxide hydrate kinetics using the experimental apparatus of the present study was carried out and the results measured at 275.2 K and 2.0 MPa are shown in Fig. 5. At each experiment three different types of water were used; (a) initially charged double distilled water, (b) water sample used immediately after dissociation, and (c) dissociated

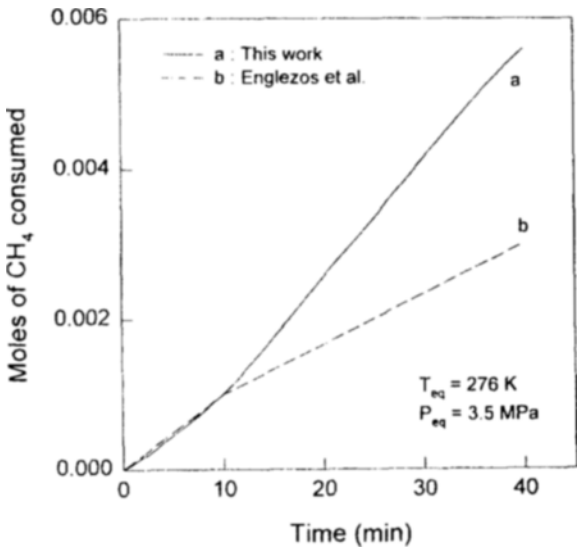

Fig. 4. Comparison of methane hydrate kinetics between this work and Englezos et al. at 276 K and 4.86 MPa.

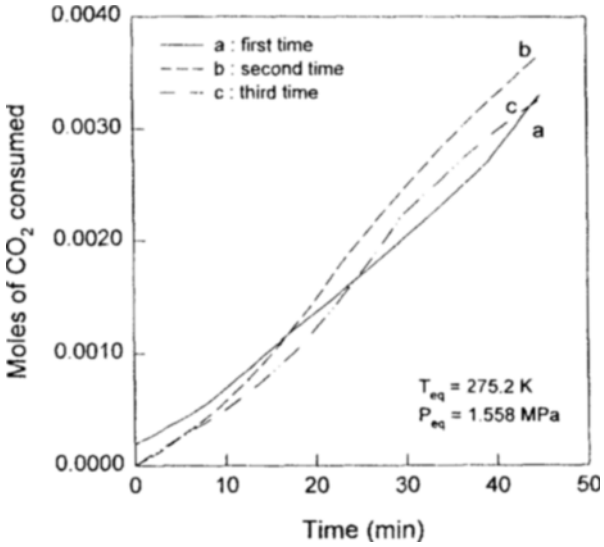

Fig. 5. Reproducibility test of carbon dioxide hydrate kinetics at 275.2 K and 2.0 MPa.

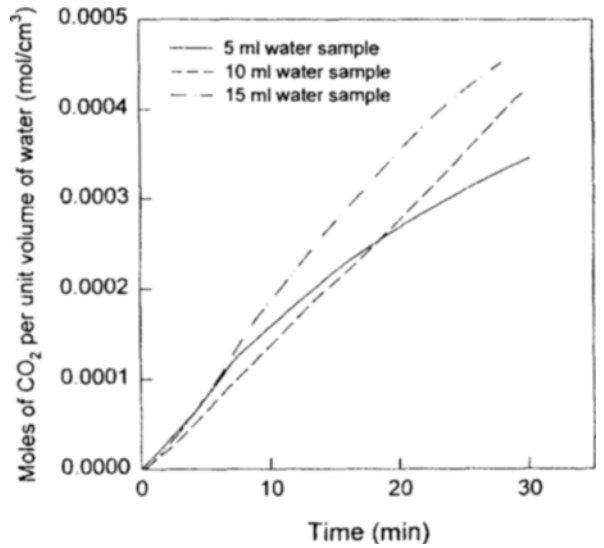

Fig. 6. Comparison of kinetics of carbon dioxide hydrate formation with respect to the variation of amount of water at 275.2 K and 2.0 MPa.

hydrate water sample left overnight before using. All three tests agreed well without the noticeable difference of carbon dioxide consumption rates. These overall results indicate that the present experimental system can reproduce the hydrate kinetic data with great confidence. This reproducibility test is important before the experimental measurement since the hydrate formation kinetic apparatus does not guarantee the reliable data.

Fig. 6 showed the comparison of the kinetic results of the carbon dioxide hydrate formation with respect to the variation of the amount of water sample charged. The consumption rates of carbon dioxide per unit volume of the water were obtained at the temperature and pressure condition of 275.2 K and 2.0 MPa. The consumption rates of carbon dioxide per unit volume of the water appeared to be almost same for all three cases. This result indicated that the consumption rate of carbon dioxide was not largely dependent on the charged amount of water samples.

The kinetic experiments of the carbon dioxide hydrate formation were performed at three different conditions, 275.2 K and 2.0 MPa, 277.2 K and 2.5 MPa, and 279.2 K and 3.5 MPa. The consumption rates were calculated by the kinetic model proposed by Englezos et al. [1987a]. The kinetic experimental results of the carbon dioxide hydrate formation were shown in Fig. 7 along with the predictive curves calculated from Englezos model at three different conditions. The data were plotted only after the turbidity point which was defined as the zero time in the Fig. 7. It was experimentally observed that the hydrate formation was not restricted to a thin layer close to the gas-liquid interface but could occur everywhere in the liquid water if supersaturation exists as a result of the dissolution process. The nature of the experimental and the fitted curves was similar for all the kinetic experiments. The estimated parameter values, K^*, at each experiment were obtained between 0.69×10^{-5} and 0.71×10^{-5} mol/m^{2}sMPa. The maximum deviation between the experimental data obtained in this work and the predictive values was found to be 7.18%. It can be said that the parameters very slightly depend on temperature since no significant chemical reaction is involved in the hydrate formation process. The hydrate kinetic model developed by Englezos et al. gave allowable predictability to the kinetic experimental data of the carbon dioxide hydrate formation of this study.

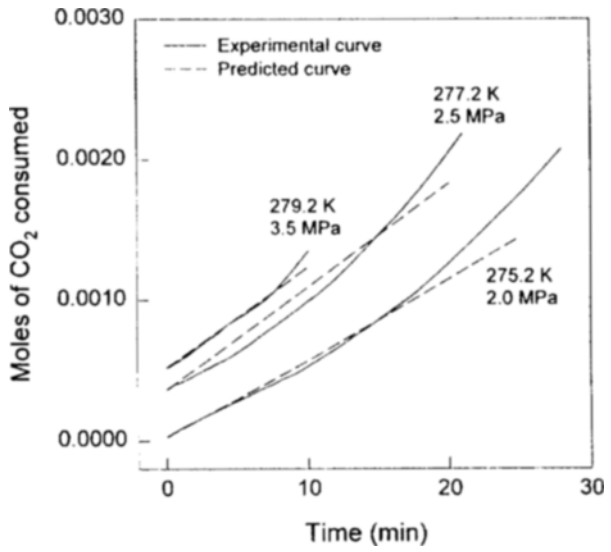

Fig. 7. Carbon dioxide hydrate kinetic results at various temperature and pressure conditions.

CONCLUSIONS

The new experimental apparatus capable of investigating the formation kinetics clathrate hydrates was developed in this study. From several preliminary tests the experimental apparatus was found to be valid to perform the kinetic experiments of clathrate hydrate formation. It is indicated that the reactor shape of this study has a better condition for methane hydrate crystal formation. The experimental kinetic data of carbon dioxide hydrate formation were firstly obtained to measure directly the volumetric flowrate of a hydrate-forming gas at several temperature and pressure conditions. It was experimentally observed that the formation of carbon dioxide hydrate was very rapid than the formation of methane hydrate was. The hydrate kinetic model developed by Englezos et al. adopted in this study was able to produce allowable estimation curves of the kinetic experimental data of carbon dioxide hydrate formation obtained in this study.

ACKNOWLEDGEMENT

This research was supported by NON DIRECTED RESEARCH FUND, Korea Research Foundation and Korea Science and Engineering Foundation.

NOMENCLATURE

a : interfacial area per unit of liquid volume [m^2/m^3]
A_{g-l} : gas-liquid interfacial area [m^2]
A_p : surface area of the particles [m^2]
c_{w0} : initial concentration of water molecules [mol/m^3]
D : diffusivity of the gas [m^2/s]
f : fugacity of the gas [MPa]
G : linear growth rate [m/s]
H : Henry's constant [MPa]
k_f : mass-transfer coefficient around the particle [m/s]
K : $4\pi\mu_2K^*$
K^* : combined rate parameter [mol/m^{2}sMPa]
L : distance between the (g – *l*) interface and the bottom of the reactor [m]
M : molecular weight of the hydrate of the form $X\cdot n_wH_2O$
n : moles of the gas consumed
n_{eq} : moles of gas dissolved at three-phase equilibrium
n_{tp} : moles of gas dissolved at the turbidity point
n_w : number of water molecules per gas molecule, 5.75 for the methane hydrate and carbon dioxide hydrate
P : pressure [MPa]
R : universal gas constant [MPam^3/molK], [J/molK]
$R_v(t)$: global reaction rate [mol/m^{3}s]
r : particle size [m]
T : temperature [K]
t : time [s]
V : volume [m^3]

v_m : molar volume of the hydrate [m^3/mol]
v_w : molar volume of water [m^3/mol]
y : distance form the (g – *l*) interface [m]
y_L : film thickness [m]

Greek Letters

α_2 : nucleation constant [nuclei/m^2s]
γ : Hatta number
Δf : driving force [MPa]
Δg : free energy change per unit volume of product [J/m^3]
μ_n : n-th moment of the crystal distribution [m^n/m^3]
μ_n^0 : initial n-th moment of the crystal distribution
ρ : hydrate density [kg/m^3]
σ : surface energy for the system hydrate-water [J/m^2]
$\phi(r, t)$: crystal size distribution [m^{-4}]

Subscripts

avg : average
b : bulk of the liquid phase
cr : critical
eq : three-phase equilibrium condition
exp : experimental conditions
g : gas phase
L : liquid phase
0 : time, 0
t : time, t
p : particle
w : water

REFERENCES

Berecz, E. and Balla-Achs, M., "Studies in Inorganic Chemistry 4; Gas Hydrates", Elsevier, Amsterdam (1983).

Dholabhai, P. D., Kalogerakis, N. and Bishnoi, P. R., "Kinetics of Methane Hydrate Formation in Aqueous Electrolyte Solutions", *Can. J. Chem. Eng.*, **71**, 68 (1993).

Englezos, P., Kalogerakis, N., Dholabhai, P. D. and Bishnoi, P. R., "Kinetics of Formation of Methane and Ethane Gas Hydrates", *Chem. Eng. Sci.*, **42**, 2647 (1987a).

Englezos, P., Kalogerakis, N., Dholabhai, P. D. and Bishnoi, P. R., "Kinetics of Gas Hydrate Formation from Mixtures of Methane and Ethane", *Chem. Eng. Sci.*, **42**, 2659 (1987b).

Hayduk, W. and Laudie, H., "Prediction of Diffusion Coefficients for Non-electrolytes in Dilute Aqueous Solutions", *AIChE J.*, **31**, 252 (1974).

Jamaluddin, A. K. M., Kalogerakis, N. and Bishnoi, P. R., "Modelling of Decomposition of a Synthetic Core of Methane Gas Hydrate by Coupling Intrinsic Kinetics with Heat Transfer Rates", *Can. J. Chem. Eng.*, **67**, 948 (1989).

Kim, H. C., Bishnoi, P. R., Heidemann, R. A. and Rizvi, S. S. H., "Kinetics of Methane Hydrate Decomposition", *Chem. Eng. Sci.*, **42**, 1645 (1987).

Lund, P. C., Shindo, Y., Fujioka, Y. and Komiyama, H., "Study of the Pseudo-Steady-State Kinetics of CO_2 Hydrate Formation and Stability", *Int. J. Chem. Kinet.*, **26**, 289 (1994).

Saji, A., Yoshida, H., Sakai, M., Tanii, T., Kamata, T. and Kitamura, H., "Fixation of Carbon Dioxide by Clathrate-Hydrate", *Energy Convers. Mamt.*, **33**, 643 (1992).

Shindo, Y., Lund, P. C., Fujioka, Y. and Komiyama, H., "Kinetics of Formation of CO_2 Hydrate", *Energy Convers. Mamt.*, **34**, 1073 (1993a).

Shindo, Y., Lund, P. C., Fujioka, Y. and Komiyama, H., "Kinetics and Mechanism of the Formation of CO_2 Hydrate", *Int. J. Chem. Kinet.*, **25**, 777 (1993b).

Sloan, E. D., Jr., "Clathrate Hydrates of Natural Gases", Mercel Dekker, Inc., New York (1990).

Teng, H., Kinoshita, M. and Masutani, S. M., "Hydrate Formation on the Surface of a CO_2 Droplet in High-Pressure, Low-Temperature Water", *Chem. Eng. Sci.*, **50**, 559 (1995).

Vysniauskas, A. and Bishnoi, P. R., "A Kinetic Study of Methane Hydrate Formation", *Chem. Eng. Sci.*, **38**, 1061 (1983).

Vysniauskas, A. and Bishnoi, P. R., "Kinetics of Methane Hydrate Formation", *Chem. Eng. Sci.*, **40**, 299 (1985).